

# Microfluidic Capture of Endothelial Colony-Forming Cells from Human Adult Peripheral Blood: Phenotypic and Functional Validation *In Vivo*

Ruei-Zeng Lin, PhD,<sup>1,2</sup> Adam Hatch, PhD,<sup>3</sup> Victor G. Antontsev, BS,<sup>3</sup>  
Shashi K. Murthy, PhD,<sup>3,4</sup> and Juan M. Melero-Martin, PhD<sup>1,2,5</sup>

**Introduction:** Endothelial colony-forming cells (ECFCs) are endothelial progenitors that circulate in peripheral blood and are currently the subject of intensive investigation due to their therapeutic potential. However, in adults, ECFCs comprise a very small subset among circulating cells, which makes their isolation a challenge.

**Materials and Methods:** Currently, the standard method for ECFC isolation relies on the separation of mononuclear cells and erythrocyte lysis, steps that are time consuming and known to increase cell loss. Alternatively, we previously developed a novel disposable microfluidic platform containing antibody-functionalized degradable hydrogel coatings that is ideally suited for capturing low-abundance circulating cells from unprocessed blood. In this study, we reasoned that this microfluidic approach could effectively isolate rare ECFCs by virtue of their CD34 expression.

**Results:** We conducted preclinical experiments with peripheral blood from four adult volunteers and demonstrated that the actual microfluidic capture of circulating CD34<sup>+</sup> cells from unprocessed blood was compatible with the subsequent differentiation of these cells into ECFCs. Moreover, the ECFC yield obtained with the microfluidic system was comparable to that of the standard method. Importantly, we unequivocally validated the phenotypical and functional properties of the captured ECFCs, including the ability to form microvascular networks following transplantation into immunodeficient mice.

**Discussion:** We showed that the simplicity and versatility of our microfluidic system could be very instrumental for ECFC isolation while preserving their therapeutic potential. We anticipate our results will facilitate additional development of clinically suitable microfluidic devices by the vascular therapeutic and diagnostic industry.

## Introduction

ENDOTHELIAL COLONY-FORMING cells (ECFCs) are a subset of endothelial progenitor cells (EPCs) that circulate in peripheral blood and are currently the subject of intensive investigation. The identification of ECFCs in human blood created a promising opportunity to noninvasively derive large quantities of autologous endothelial cells for therapeutic use. Indeed, ECFCs have an enormous expansion capacity in culture.<sup>1</sup> In addition, the therapeutic potential of ECFCs has been demonstrated using numerous preclinical *in vivo* models. Initial demonstrations included endothelialization of cardiovascular grafts. For instance, Kaushal *et al.* showed that decellularized porcine iliac vessels seeded with autologous ovine ECFCs and implanted as a carotid interposition graft in

sheep had adequate patency and arterial function *in vivo* for several months.<sup>2</sup> The antithrombotic properties of human ECFCs were corroborated in subsequent studies using additional vascular grafts.<sup>3</sup> *In vivo* studies have also demonstrated the inherent vasculogenic properties of ECFCs.<sup>1</sup> Following transplantation into mice in combination with perivascular cells, studies have repeatedly shown that ECFCs self-assemble into long-lasting microvascular networks that anastomose with the host vasculature.<sup>4,5</sup> These newly formed ECFC-lined microvessels are similar to normal vessels in several respects, including nonthrombogenicity, blood flow, regulation of macromolecule permeability, and capacity to induce leukocyte-endothelial interactions in response to cytokine activation.<sup>4</sup> Thus, taken together, ECFCs are ideally suited for autologous vascular therapies.

<sup>1</sup>Department of Cardiac Surgery, Boston Children's Hospital, Boston, Massachusetts.

<sup>2</sup>Department of Surgery, Harvard Medical School, Boston, Massachusetts.

<sup>3</sup>Department of Chemical Engineering and <sup>4</sup>Barnett Institute of Chemical and Biological Analysis, Northeastern University, Boston, Massachusetts.

<sup>5</sup>Harvard Stem Cell Institute, Cambridge, Massachusetts.

Beside their therapeutic potential, mounting evidence indicates that variations of ECFC levels are likely associated with various pathologies,<sup>6–12</sup> and thus there is also increasing interest in accounting levels of ECFCs for diagnostic purposes.

ECFCs comprise a very small population among circulating cells, which makes their isolation a challenge. Indeed, consensus holds that ECFCs are relatively abundant in umbilical cord blood, but exceedingly rare in adult peripheral blood.<sup>13,14</sup> For instance, Yoder *et al.* estimated normal ECFC levels as 0.017 per million blood mononuclear cells (MNCs) in healthy adults aged 19–50 years, which is ~15-fold lower than in cord blood.<sup>13,15</sup> Given this low occurrence, it is not surprising that several studies have reported an apparent absence of ECFCs in a substantial proportion (>25%) of healthy and nonhealthy adults.<sup>3</sup> Inducing ECFC mobilization could eliminate this uncertainty; however, the mechanisms by which ECFCs are mobilized into circulation are still unknown. Meanwhile, efforts are increasingly being directed toward developing more reliable methods for ECFC isolation in adults.

Currently, the standard method for ECFC isolation is based on the colony-forming ability of these cells and follows a technique originally established by Lin *et al.* for blood outgrowth endothelial cells.<sup>16</sup> This method for ECFC isolation relies on the separation of MNCs and erythrocyte lysis, steps that are time consuming and prone to increased cell loss. However, the paucity of circulating ECFCs and the lack of a unique set of distinctive cellular markers have hampered the development of alternative flow cytometry or immunological isolation techniques. For instance, a recent study by Mund *et al.* demonstrated prospective detection of circulating ECFCs (CD31<sup>bright</sup>/CD34<sup>+</sup>/CD45<sup>-</sup>/AC133<sup>-</sup> cells) by polychromatic flow cytometry, but the approach was found detrimental to the actual recovery of viable ECFCs.<sup>17</sup> Indeed, flow cytometry can exert acute hydrodynamic forces and induce apoptosis on processed cells.<sup>18</sup> Additional immunomagnetic-based techniques have been pursued for the selection of ECFCs, although with mixed results.<sup>19</sup> Moreover, these techniques require laborious and time-intensive steps associated with the need to (1) exclude interfering cell populations (specifically red blood cells) and (2) attach fluorescent or magnetic tags to one or more cell types.<sup>20</sup> Thus, the search for alternative strategies that can render adult ECFCs from unmanipulated blood remains an active area of research.

Microfluidic cell separation systems are of particular interest in clinical and biological applications where samples must be processed efficiently and rapidly.<sup>21</sup> In recent years, we developed a novel disposable microfluidic platform containing antibody-functionalized degradable hydrogel coatings that is ideally suited for capturing low-abundance circulating cells from untreated blood<sup>22–24</sup> and tissue digest.<sup>25</sup> Indeed, we demonstrated efficient microfluidic detection of CD34<sup>+</sup> cells from whole blood in healthy subjects<sup>24,26</sup> as well as in patients with pulmonary arterial hypertension, an approach that eliminated sample preprocessing.<sup>27</sup> In this study, we reason that this microfluidic approach can also be instrumental in isolating rare circulating ECFCs. We have examined the feasibility of capturing ECFCs from whole peripheral blood in four adult volunteers and conducted preclinical experiments to validate the phenotypical and functional properties of the captured ECFCs, including the ability to form microvascular networks *in vivo*.

## Materials and Methods

### Microfluidic device design and fabrication

The design and fabrication of the micropost array microfluidic devices followed previously described soft lithography techniques.<sup>22</sup> First, a negative master was fabricated and assembled at the George J. Kostas Nanoscale Technology and Manufacturing Research Center at Northeastern University using conventional photolithography techniques. Briefly, a silicon wafer was coated with SU-8 50 photoresist to a thickness of ~50 μm. With the transparency overlaid, the wafer was exposed to 365 nm, 11 mW/cm<sup>2</sup> UV light from a Q2001 mask aligner (Quintel Co.). The unexposed photoresist was then removed using the SU 8 developer. Feature height was verified using a Dektak surface profiler (Veeco Instruments). Postarray devices consisting of 100-μm diameter posts with a gap, edge-to-edge distance of 50 μm were fabricated. Posts were arranged in a hexagonal pattern, where three adjacent posts form an equilateral triangle pattern. The overall dimension of the device was 5×7×0.05 mm. To form the polymeric chambers, poly(dimethylsiloxane) (PDMS, Sylgard 184; Dow Corning) elastomer was mixed (10:1 ratio) and poured onto a negative master, degassed, and allowed to cure overnight. PDMS replicas were then removed; inlet and outlet holes were punched with a 19-G blunt-nosed needle. Replicas and glass microscope slides (25×75×1 mm<sup>3</sup>) were then exposed to oxygen plasma and placed in contact to bond irreversibly. Micropost surface modification was carried out as previously described.<sup>24</sup> Briefly, poly(ethylene glycol) and alginate (Sigma) were mixed in an equal molar ratio, combined with EDC [1-ethyl-3-(3-dimethylaminopropyl)carbodiimide hydrochloride] and sulfo-NHS (N-hydroxysuccinimide) (Fisher Scientific). The mixture was then injected by hand into the microfluidic devices and allowed to incubate for 60 min. The bulk gel was then removed from the device by flowing 2-(4-morpholino) ethanesulfonic acid (MES) buffer at 10 μL/min. The remaining gel was solidified by injection of 100 mM calcium chloride solution at 10 μL/min. Mouse anti-human CD34 antibody (Santa Cruz Biotechnology) at a concentration of 10 μg/mL was combined with EDC and sulfo-NHS, injected by hand, and allowed to incubate for 30 min.

### Blood collection

Adult peripheral blood (12 mL) was collected from volunteer donors by venipuncture in accordance with an Institutional Review Board-approved protocol (Northeastern University) and with informed consent according to the Declaration of Helsinki. Blood samples were collected in heparinized tubes (Becton Dickinson). Each sample was split into two (6 mL each); one half was processed following the standard ECFC isolation method and the other half using our microfluidic device (Fig. 1).

### Standard ECFC isolation method

Blood (6 mL) was diluted 1:1 with the isolation buffer (phosphate buffered saline [PBS], 0.6% ACD-A, 0.5% bovine serum albumin [BSA]) in a centrifuge tube and was overlaid onto an equivalent volume of the Ficoll-Paque Plus (Amersham Pharmacia). Cells were centrifuged for 15 min at room temperature at 1467 g. MNCs were gently collected,

washed two times with the isolation buffer, diluted 1:1 with ammonium chloride solution (StemCell Technologies), and incubated for 5 min on ice for erythrocyte lysis. MNCs were then washed two times with the isolation buffer and cultured on 1% gelatin-coated plates using ECFC medium: EGM-2 (except for hydrocortisone; Lonza) supplemented with 20% fetal bovine serum (FBS), and 1× glutamine–penicillin–streptomycin (Invitrogen). Unbound cells were removed at 48 h and the bound fraction maintained in ECFC medium, with media being replenished every 2–3 days.

#### *Microfluidic ECFC isolation method*

Whole blood (6 mL) was directly flowed through 20 parallel microfluidic devices with anti-human CD34 antibody-functionalized posts at 5  $\mu$ L/min using a PHD2000 syringe pump (Harvard Apparatus). The blood was then rinsed from the device using MES buffer at a flow rate of 10  $\mu$ L/min to a total volume of 100  $\mu$ L (10 min) followed by an injection of a 50 mM solution (100  $\mu$ L; 10  $\mu$ L/min) of ethylene diamine tetraacetic acid (EDTA) in PBS (Fisher Scientific) to elute cells. The eluted cell fraction was then cultured on 1% gelatin-coated plates using ECFC medium. Unbound cells were removed at 48 h and the bound fraction maintained in ECFC medium, with media being replenished every 2–3 days.

#### *ECFC culture*

ECFC colonies were identified as well-circumscribed monolayers of >50 cells with typical cobblestone morphology. ECFC colonies were enumerated on day 28 by visual inspection using an inverted microscope. At confluence, ECFCs were purified using anti-human CD31 antibody-coated beads (DynaL Biotech) as previously described.<sup>1</sup> CD31-selected ECFCs were routinely subcultured on 1% gelatin-coated plates using ECFC medium. ECFCs are hereafter referred to as std-ECFCs (standard isolation method) and mf-ECFCs (microfluidic isolation method). Both std-ECFCs and mf-ECFCs were used between passages 4–8 in all our studies.

#### *Flow cytometry*

Flow cytometry analyses were carried out by labeling cells with either phycoerythrin (PE)-conjugated mouse anti-human CD31 (1:100; Ancell), PE-conjugated mouse anti-human CD90, fluorescein isothiocyanate (FITC)-conjugated mouse anti-human CD45, FITC-mouse IgG1, or PE-mouse IgG1 antibodies (1:100; BD Biosciences). Antibody labeling was carried out for 20 min on ice followed by three washes with 1% BSA, 0.2 mM EDTA in PBS, and resuspended in 1% paraformaldehyde in PBS. Samples were analyzed with a Guava easyCyte 6HT/2L flow cytometer (Millipore Corporation) and the FlowJo software (Tree Star, Inc.).

#### *Immunofluorescence staining*

Immunofluorescence staining was carried out using mouse anti-human CD31 (1:200; DakoCytomation), mouse anti-human von Willebrand factor (vWF) (1:200; DakoCytomation), and goat anti-human VE-cadherin (1:200; Santa Cruz Biotechnology) antibodies, followed by FITC-conjugated secondary antibodies (1:200; Vector Laboratories) and Vectashield mounting medium with DAPI (Vector Laboratories).

#### *Proliferation assay*

ECFCs were seeded in triplicate onto fibronectin-coated (10  $\mu$ g/mL) 24-well plates at a density of  $5 \times 10^3$  cell/cm<sup>2</sup> using basal medium (EBM-2, 5% FBS). Plating efficiency was determined at 24 h. Cells were then treated for 48 h using basal medium in the presence or absence of either 10 ng/mL vascular endothelial growth factor A (VEGF-A) or 1 ng/mL basic fibroblast growth factor (bFGF) (R&D Systems). Cells were quantified under a fluorescent microscope after DAPI staining using the ImageJ analysis software (National Institutes of Health); results were normalized to cell number obtained in basal medium.

#### *Scratch assay*

The scratch assay was performed in confluent cultures of ECFCs plated on six-well plates. Scratch wounds were generated across each well using a pipette tip. Cells were then treated for 14 h using basal medium in the presence or absence of 10 ng/mL VEGF-A or 1 ng/mL bFGF. Scratch size was measured after 14 h under a phase contrast microscope.

#### *Tube formation assay*

ECFCs were seeded on Matrigel-coated plates at a density of  $2 \times 10^4$  cell/cm<sup>2</sup> and incubated for 24 h in ECFC medium. Cells were stained with cell viability dye (Invitrogen) to distinguish viable from dead cells. The total length of ECFC-lined cords was measured using the ImageJ software.

#### *Upregulation of leukocyte adhesion molecules*

ECFC monolayers cultured on six-well plates were challenged with or without 10 ng/mL of tumor necrosis factor- $\alpha$  (TNF- $\alpha$ ; R&D Systems) for 5 h. Afterward, the leukemia cell line HL-60 ( $2 \times 10^6$  cells) was added and incubated at 4°C on a rocking platform for 45 min. Bound leukocytes were visualized using a phase contrast microscope and quantified with the ImageJ software. Additionally, leukocyte adhesion molecules were analyzed by flow cytometry using PE-conjugated antibodies against human E-selectin and intercellular adhesion molecule 1 (ICAM-1) (1:100; BD Biosciences).

#### *In vivo vasculogenic assay*

Six-week-old athymic nu/nu mice were purchased from Massachusetts General Hospital. Mice were housed in compliance with Boston Children's Hospital guidelines, and all animal-related protocols were approved by the Institutional Animal Care and Use Committee. Vasculogenesis was evaluated *in vivo* using our xenograft model as previously described.<sup>28,29</sup> Briefly, ECFCs and human bone marrow-derived mesenchymal stem cells (MSCs) (two million total; 2:3 ECFC/MSC ratio) were resuspended in 200  $\mu$ L of collagen-fibrin gel and the mixture was subcutaneously injected. All experiments were carried out in four mice.

#### *Histology and immunohistochemistry*

Implants were removed from euthanized mice 7 days after implantation, fixed in 10% buffered formalin overnight, embedded in paraffin, and sectioned (7- $\mu$ m-thick). Hematoxylin and eosin (H&E) stained sections were examined for

the presence of blood vessels containing red blood cells. Microvessel density (vessels/mm<sup>2</sup>) was reported as the average number of erythrocyte-filled vessels in sections from the middle of the implants. For immunohistochemistry, sections were deparaffinized, and antigen retrieval was carried out by heating the sections in Tris-EDTA buffer (10 mM Tris-Base, 2 mM EDTA, 0.05% Tween-20, pH 9.0). Sections were blocked for 30 min in 5–10% blocking serum and incubated with primary antibodies for 1 h at room temperature. The following primary antibodies were used: mouse anti-human CD31 (1:50; DakoCytomation, M0823 Clone JC70A), mouse anti-human  $\alpha$ -smooth muscle actin ( $\alpha$ -SMA) (1:200; Sigma-Aldrich, A2547 Clone 1A4), and mouse IgG (1:50; DakoCytomation). Horseradish peroxidase-conjugated mouse secondary antibody (1:200; Vector Laboratories) and 3,3'-diaminobenzidine were used for detection of human CD31, followed by hematoxylin counterstaining and Permount mounting. Fluorescent staining was performed using rhodamine-conjugated ulex europaeus agglutinin 1 (UEA-1) (20  $\mu$ g/mL) and FITC-conjugated secondary antibodies (1:200; Vector Laboratories) followed by DAPI counterstaining.

### Microscopy

Images were taken using an Axio Observer Z1 inverted microscope and the AxioVision Rel. 4.8 software (Carl Zeiss). Phase microscopy images were taken with an AxioCam MRm camera and 5 $\times$ /0.16 or 10 $\times$ /0.3 objective lens. Fluorescent images were taken with an ApoTome.2 Optical sectioning system (Carl Zeiss) and 20 $\times$ /0.8 or 40 $\times$ /1.4 oil objective lens. Nonfluorescent images were taken with an AxioCam MRc5 camera using a 40 $\times$ /1.4 objective oil lens.

### Statistical analyses

Data were expressed as mean  $\pm$  standard error of the mean. Means were compared using unpaired Student's *t*-tests. Comparisons between multiple groups were performed by ANOVA followed by Bonferroni post-test analysis. All statistical analyses were performed using the GraphPad Prism v.5 software (GraphPad Software, Inc).  $p < 0.05$  was considered statistically significant.

## Results

### Microfluidic capture of ECFCs from unprocessed whole blood

Adult peripheral blood (12 mL) was collected from four separate healthy volunteers in heparinized tubes. Each sample was split into two (6 mL each) and each half was processed following either the standard ECFC isolation method or our microfluidic devices (Fig. 1). The standard isolation method required several initial blood processing steps (namely, density gradient centrifugation, erythrocyte lysis, and various cell washes) to obtain the erythrocyte-free MNC fraction. In contrast, the microfluidic devices did not require initial processing and used heparinized, but otherwise, unprocessed whole blood. The microfluidic devices captured CD34<sup>+</sup> cells from whole blood, which were then eluted and plated in culture for comparative studies with cells obtained with the standard methodology. Processing time for the microfluidic

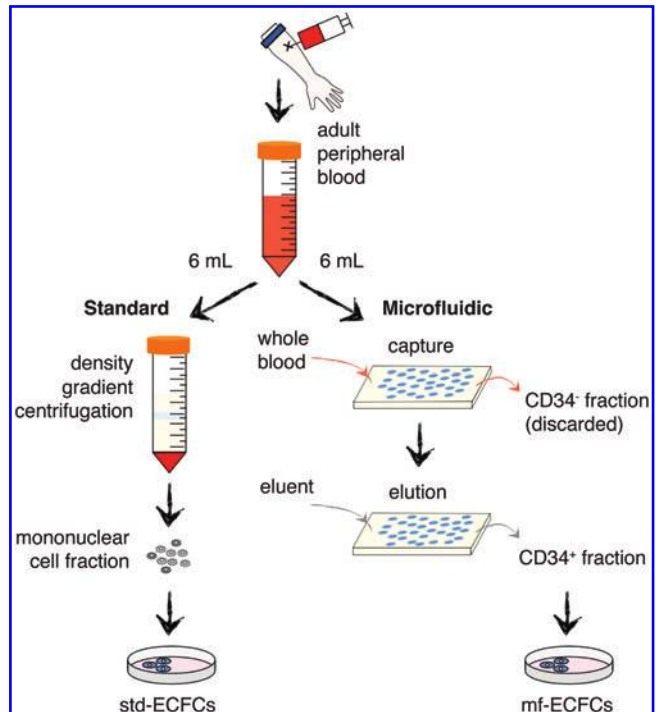


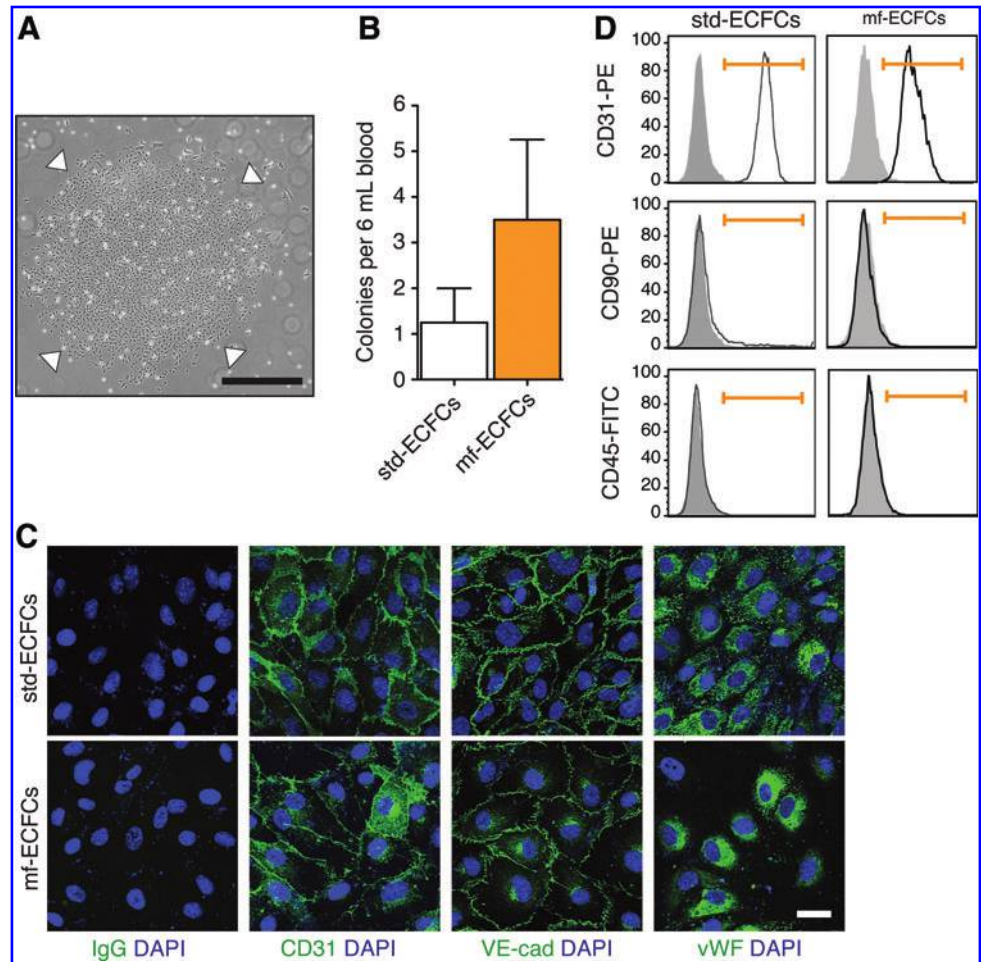
**FIG. 1.** Microfluidic device for the capture of endothelial colony-forming cells (ECFCs): diagram of study design. Peripheral blood from adult human ( $n=4$ ) was divided into two groups (6 mL each) and processed by either standard centrifugal method or microfluidic capture. Enriched mononuclear cell fraction or captured CD34<sup>+</sup> cells were cultured separately in ECFC medium to enumerate the emergence of ECFC colonies. ECFCs obtained from standard and microfluidic methods are referred as std-ECFCs and mf-ECFCs, respectively. Color images available online at [www.liebertpub.com/tec](http://www.liebertpub.com/tec)

approach was  $\sim 60$  min, which was comparable to the processing time required in the standard method.

We examined the appearance of ECFC colonies in cultures fed with endothelial growth medium. ECFCs were identified as outgrown colonies containing  $> 50$  endothelial cells (Fig. 2A). The majority of the colonies emerged in culture between 2 and 4 weeks, which is consistent with previous reports.<sup>1</sup> The abundance of ECFCs in each blood sample was determined after 4 weeks in culture (Fig. 2B). The number of ECFCs obtained with the microfluidic method was  $3.5 \pm 1.8$  colonies per 6 mL ( $n=4$  subjects), which was superior, although statistically similar, to the abundance found using the standard method ( $1.3 \pm 0.8$  colonies per 6 mL of blood) ( $p=0.28$ ). Analysis of each individual sample revealed that the microfluidic isolation method rendered more ECFC colonies in three of the four subjects sampled, confirming that the initial microfluidic technique was in itself not detrimental to the subsequent differentiation of CD34<sup>+</sup> cells into ECFCs.

ECFCs, referred to herein as std-ECFCs (standard isolation method) and mf-ECFCs (microfluidic isolation method), were allowed to grow and were then purified by expression of CD31. The endothelial phenotype of CD31-selected mf-ECFCs was verified through their expression of CD31 and VE-cadherin at the cell–cell borders, and the expression of

**FIG. 2.** Microfluidic capture of ECFCs from unprocessed whole blood. **(A)** Phase contrast image of a representative ECFC colony from a microfluidic capture. *Arrowheads* indicate the border of the colony. Scale bar represents 500  $\mu\text{m}$ . **(B)** Total number of ECFC colonies in 6 mL of peripheral blood isolated by standard (std-ECFCs;  $n=4$ ) and microfluidic (mf-ECFCs;  $n=4$ ) methods. **(C)** Indirect immunofluorescent staining of std-ECFCs and mf-ECFCs for the expression of CD31, VE-cadherin, and von Willibrand factor (vWF). Mouse IgG served as negative control. Cell nuclei were counterstained with DAPI. Scale bar represents 50  $\mu\text{m}$ . **(D)** Flow cytometric analysis of std-ECFCs and mf-ECFCs for CD31, CD90, and CD45 (*black line histograms*). Isotype-matched controls are overlaid in *solid gray histograms*. Color images available online at [www.liebertpub.com/tec](http://www.liebertpub.com/tec)



vWF in a punctuate pattern in the cytoplasm (Fig. 2C). Flow cytometry confirmed uniform expression of CD31 and negative expression of mesenchymal marker CD90 and pan-hematopoietic marker CD45 (Fig. 2D). In addition, we demonstrated that culture-expanded mf-ECFCs were highly pure ( $>97\%$  CD31 $^{+}$ ), with low to nondetectable hematopoietic (CD45 $^{+}$ ) or mesenchymal (CD90 $^{+}$ ) contaminants (Fig. 2D). Collectively, this characterization revealed that mf-ECFCs were phenotypically highly similar to std-ECFCs.

#### In vitro validation of ECFC function

To assess ECFC function, we performed several *in vitro* functional assays (Fig. 3). First, we tested the ability of mf-ECFCs to upregulate leukocyte adhesion molecules in response to an inflammatory cytokine (TNF- $\alpha$ ). E-selectin and ICAM-1 were low to undetectable in untreated mf-ECFCs (Fig. 3A). However, as expected, both adhesion molecules were markedly upregulated after 5 h incubation with TNF- $\alpha$  (Fig. 3A). This upregulation resulted in increased adhesion of HL-60 leukocytes (Fig. 3B). Also, quantitative analysis of the increase in leukocyte adhesion upon TNF- $\alpha$  exposure showed no statistically significant differences ( $p=0.87$ ) between mf-ECFCs (71-fold) and std-ECFCs (67-fold), which indicated that microfluidic isolation did not alter the physiological proinflammatory responsiveness of ECFCs.

Next, we examined the response of mf-ECFCs to proangiogenic growth factors. First, using a standard proliferation assay, we found that both VEGF and bFGF induced ECFC mitogenesis. The number of mf-ECFCs after 48 h exposure to each growth factor was significantly higher than in cultures with basal medium (3.3-fold for VEGF and 5.8-fold for bFGF) (Fig. 3C). In addition, the proliferative response of mf-ECFCs was statistically similar to that of std-ECFCs for both VEGF ( $p=0.25$ ) and bFGF ( $p=0.68$ ) (Fig. 3C). Similarly, exposure to VEGF and bFGF significantly increased the capacity of mf-ECFCs to reendothelialize scratched monolayers (2.8-fold increase for VEGF and 2-fold for bFGF) (Fig. 3D). This migratory response of mf-ECFCs was statistically similar to that of std-ECFCs for both VEGF ( $p=0.41$ ) and bFGF ( $p=0.62$ ) (Fig. 3D).

Lastly, we evaluated the ability of mf-ECFCs to form tubular structures *in vitro*. Indeed, we found that mf-ECFCs formed extensive networks of capillary-like structures when cultured on top of Matrigel (Fig. 3E). The extent of these vascular networks was statistically similar between mf-ECFCs (total tube length of  $2.2 \pm 0.1 \text{ mm/mm}^2$ ) and std-ECFCs ( $2.1 \pm 0.1 \text{ mm/mm}^2$ ) (Fig. 3E;  $p=0.60$ ).

#### Validation of ECFC vasculogenic function in mice

A critical functional validation for ECFCs is the ability to form perfused vascular networks *in vivo*. We examined

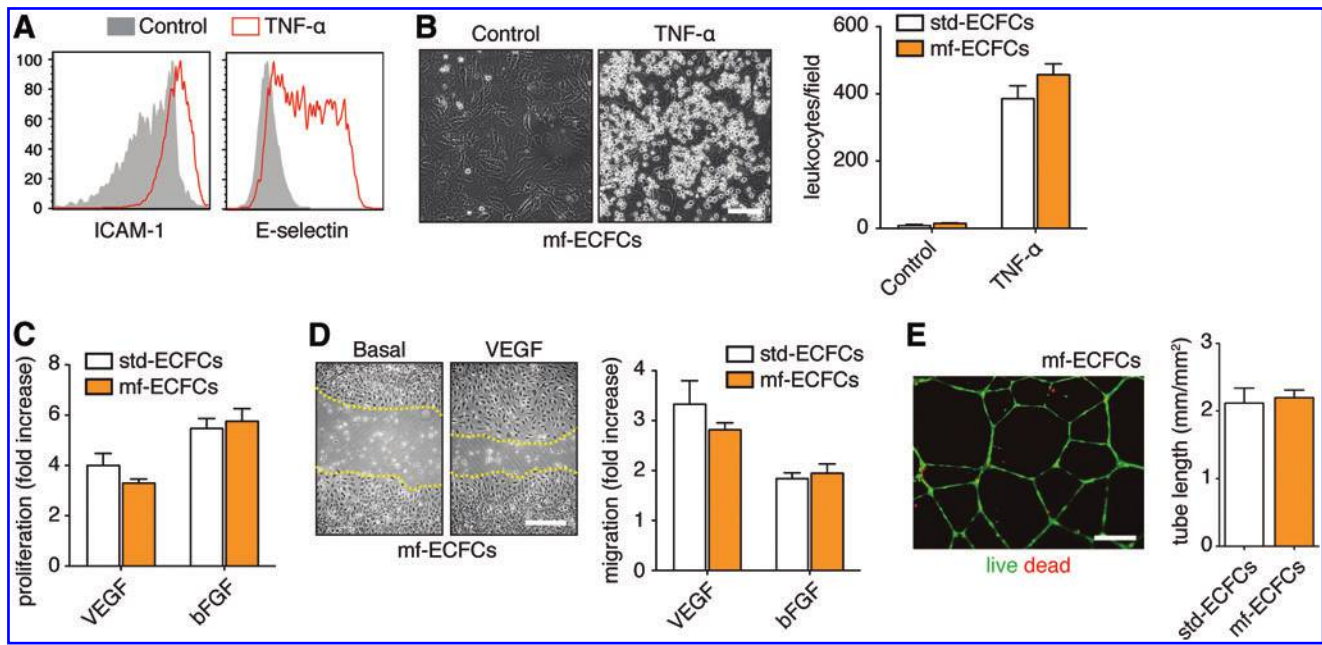


**FIG. 3.** *In vitro* assessment of ECFC function. (A) Flow cytometric analysis of mf-ECFCs for upregulation of E-selectin and intercellular adhesion molecule 1 (ICAM-1) in response to tumor necrosis factor- $\alpha$  (TNF- $\alpha$ ). Line histograms represent cells stimulated with TNF- $\alpha$ , whereas solid gray histograms represent untreated controls. (B) Representative images of mf-ECFCs with an increased number of bound leukocytes after TNF- $\alpha$  treatment compared with untreated control (scale bar: 200  $\mu$ m). Quantification of bound leukocytes per image field for each of ECFC group. (C) Cell proliferation after 48 h in response to vascular endothelial growth factor A (VEGF-A) (10 ng/mL) and basic fibroblast growth factor (bFGF) (1 ng/mL). Cell number was normalized to those obtained in basal medium. (D) Cell migration in response to VEGF-A (10 ng/mL) and bFGF (1 ng/mL) assessed by the scratch assay. Representative images of scratched mf-ECFC monolayers after 14 h in basal and VEGF-A-containing medium. Dashed lines delineate the scratches (scale bar: 500  $\mu$ m). Migration was quantified as percentage of scratch closure after 14 h and compared with closure obtained in basal medium. (E) Representative image of capillary-like network assembled by mf-ECFCs on Matrigel-coated plates (scale bar: 500  $\mu$ m). Green and red fluorescence indicate viable and dead cells, respectively. Total tube length per unit of area was quantified at 24 h. Color images available online at [www.liebertpub.com/tec](http://www.liebertpub.com/tec)

the vasculogenic potential of both mf-ECFCs and std-ECFCs using our xenograft model of human vascular cell transplantation into athymic immunodeficient nude mice.<sup>4</sup> Briefly, ECFCs and MSCs ( $2 \times 10^6$  in total; ECFC:MSC ratio = 2:3) were resuspended in 200  $\mu$ L of collagen-fibrin gel and the mixture subcutaneously injected into nude mice (Fig. 4A). H&E-stained sections from grafts explanted at day 7 revealed the presence of extensive networks of perfused blood vessels in implants with mf-ECFCs (arrowheads = erythrocyte-containing vessels in Fig. 4B). Quantitative evaluation of microvessel density demonstrated no statistical difference between grafts that contained mf-ECFCs ( $159.2 \pm 39.6$  vessel/mm<sup>2</sup>) and those containing std-ECFCs ( $80.5 \pm 27.7$  vessel/mm<sup>2</sup>) (Fig. 4C;  $p = 0.18$ ). Moreover, microvessels were uniformly distributed throughout the graft and their lumens were lined by human mf-ECFCs, as confirmed by immunohistochemical staining with a human-specific CD31 antibody (Fig. 4D). Microvessels also stained positively for UEA-1, a lectin that specifically binds human (but not murine) endothelial cells (Fig. 4E). In addition, ECFC-lined microvessels had extensive perivascular coverage at day 7 with cells expressing  $\alpha$ -SMA (Fig. 4E), which indicated vascular stability. Importantly, quantitative evaluation of the percentage of human vessels with complete perivascular coverage demonstrated no statistical difference between grafts that con-

tained mf-ECFCs ( $91.9\% \pm 2.2\%$  of the vessel) and those containing std-ECFCs ( $88.1\% \pm 2.8\%$ ) (Fig. 4F;  $p = 0.35$ ).

Collectively, we demonstrated that mf-ECFCs had robust *in vivo* vasculogenic potential. Our characterization confirmed that the phenotype of mf-ECFCs corresponded to that of bona fide endothelial cells. Indeed, mf-ECFCs responded to various stimuli in culture as expected and were functionally highly similar to std-ECFCs both *in vitro* and *in vivo*.

## Discussion

The present study demonstrates that human ECFCs can effectively be isolated from adult peripheral blood by virtue of their CD34 expression using microfluidics. Key findings documented in this study relate to the phenotypic and functional validation of the captured mf-ECFCs. First, we showed that our microfluidic isolation technique yielded statistically similar number of ECFCs than the standard isolation method, which is based on density gradient centrifugation and MNC derivation. Importantly, the comparison between the standard and microfluidic methods was done side-by-side by splitting into two each sample of peripheral blood from each volunteer subject. Second, we showed that mf-ECFCs uniformly expressed endothelial cell markers (CD31, vWF, and VE-cadherin), but not hematopoietic (CD45) and mesenchymal (CD90) markers, and that mf-ECFC cultures were highly

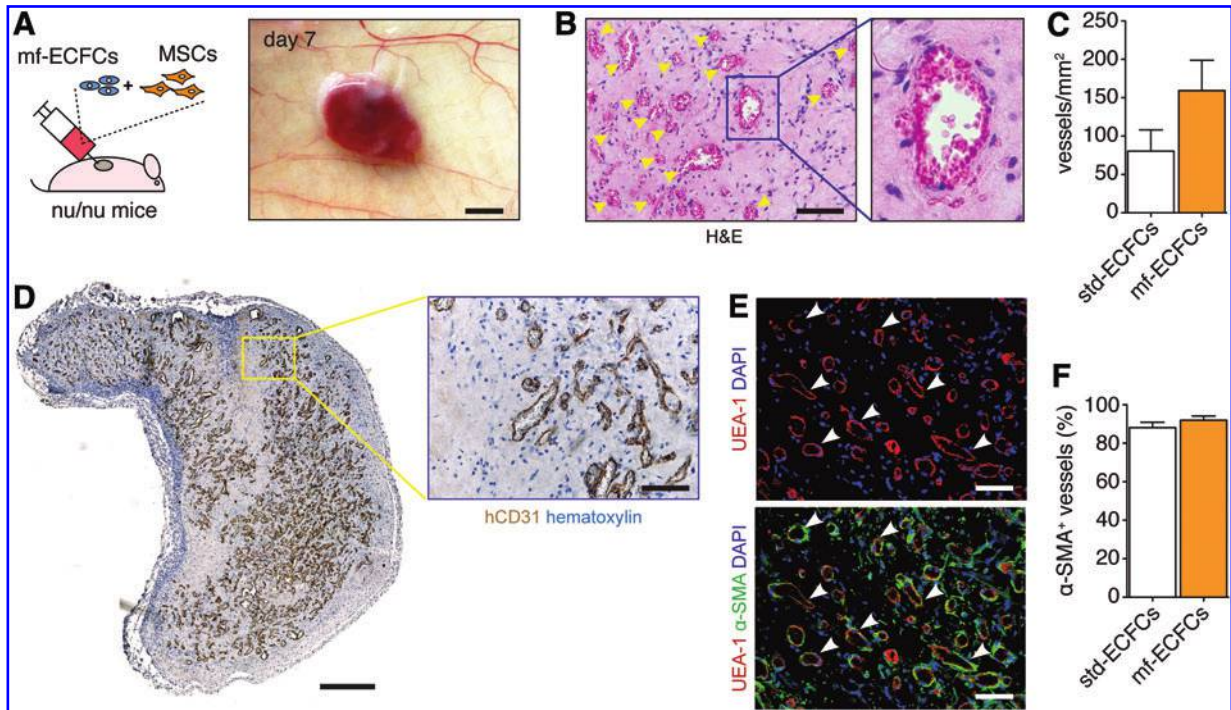


**FIG. 4.** Validation of ECFC vasculogenic function in mice. (A) mf-ECFCs and mesenchymal stem cells (MSCs) were embedded in collagen-fibrin gel and the mixture injected subcutaneously into nude mice. Macroscopic view of one representative implant at the site of implantation after 7 days (scale bar: 2 mm). (B) Histological identification of microvascular vessels in mf-ECFC-containing explants. Representative hematoxylin and eosin (H&E)-stained section of one mf-ECFC explant revealing the presence of numerous luminal structures containing murine erythrocytes (arrowheads) (scale bar: 100  $\mu$ m). (C) Microvessel density was quantified at day 7 in both groups ( $n = 3$  each). (D) Immunohistochemical staining using an anti-human specific CD31 (hCD31) antibody revealed that the majority of the blood vessels were lined by human mf-ECFCs. Cell nuclei were counterstained with hematoxylin (scale bar: 500  $\mu$ m in left panel and 100  $\mu$ m in right panel). (E) Representative immunofluorescent panels from an implant seeded with mf-ECFCs. Microvessels were examined by double staining using UEA-1 (red) and  $\alpha$ -smooth muscle actin ( $\alpha$ -SMA; green). Nuclei were counterstained with DAPI. Microvessels lined by human ECFCs were identified as UEA-1<sup>+</sup> lumens and the majority had complete perivascular coverage ( $\alpha$ -SMA<sup>+</sup>) (arrowheads) (scale bar: 100  $\mu$ m). (F) Percentage of human UEA-1<sup>+</sup> microvessels covered by  $\alpha$ -SMA<sup>+</sup> perivascular cells in both std-ECFCs and mf-ECFCs groups ( $n = 3$ ). Color images available online at [www.liebertpub.com/tec](http://www.liebertpub.com/tec)

pure (>97%) and the presence of other cellular contaminants (namely, hematopoietic and mesenchymal cells) was negligible. Third, we demonstrated that culture-expanded mf-ECFCs robustly displayed endothelial properties and functions, as confirmed by (1) binding of UEA-1 lectin; (2) *in vitro* capillary-like network formation ability; (3) proliferative and migratory responses to angiogenic growth factors (VEGF, bFGF); and (4) upregulation of leukocyte adhesion molecules (E-selectin, ICAM-1) upon exposure to an inflammatory cytokine (TNF- $\alpha$ ) and subsequent increase in leukocyte binding. Lastly, we showed that culture-expanded mf-ECFCs had robust *in vivo* vasculogenic potential. Without exception, all mf-ECFCs tested rapidly generated an extensive network of human blood vessels following subcutaneous transplantation with MSCs into immunodeficient mice. Moreover, mf-ECFCs specifically lined the lumens of the newly formed microvessels, whereas MSCs occupied perivascular positions. Importantly, we found no differences between std-ECFCs and mf-ECFCs in terms of the ability to form microvessels with extensive perivascular coverage. Collectively, this characterization revealed that mf-ECFCs were phenotypically and functionally highly similar to std-ECFCs.

A critical aspect of our study was the need for well-defined cellular phenotypes. Over the last decade, a growing body of studies has substantiated the specific phenotypic characteristics of ECFCs. However, ECFCs are widely regarded as a subset of circulating EPCs, and given that multiple subpopulations of cells have been embraced under the general definition of EPCs, phenotype validation is particularly important when contemplating the use of ECFCs.<sup>30,31</sup> For instance, early studies identified putative EPCs as circulating cells that were derived from the bone marrow and coexpressed a combination of endothelial and stem cell markers, including CD34, CD133, and VEGFR-2.<sup>32,33</sup> However, subsequent studies over the last decade revealed that most of the cells originally defined as EPC are closely related to myelomonocytic hematopoietic cells at various stages of differentiation.<sup>30,34</sup> These hematopoietic EPCs (also referred to as early EPCs and as angiogenic EPCs<sup>14</sup>) serve as paracrine mediators and play an important role in neovascularization and vascular repair *in vivo*; however, hematopoietic EPCs do not give rise to endothelial progeny. Meanwhile, consensus holds that ECFCs (also referred to as late EPCs<sup>35</sup> and as circulating outgrowth endothelial cells<sup>16</sup>) are non-hematopoietic EPCs with bona fide endothelial properties and

although the exact origin of ECFCs remains to be clarified, their capacity to function as structural endothelial cells *in vivo* has been repeatedly demonstrated by multiple independent laboratories.<sup>1,5,15,36–38</sup> Thus, despite the terminology conundrum that has complicated this field of research for over a decade, the functional differences between the various subpopulations of EPCs are now widely recognized.<sup>31,39</sup> Nevertheless, performing rigorous and distinctive phenotypic characterizations remains a critical issue in the field of EPC research. In this study, we unambiguously demonstrated that mf-ECFCs captured with our microfluidic device were phenotypically and functionally identical to std-ECFCs derived by the standard method from the same volunteer subjects, including their capacity to form vascular networks *in vivo*. Moreover, we showed that none of our mf-ECFCs expressed the pan-hematopoietic marker CD45, confirming the unequivocal distinction between our mf-ECFCs and other potential hematopoietic EPCs.

Our study highlighted several practical aspects inherent to microfluidic systems that could be advantageous when considering translational or clinical applications. We first demonstrated that the actual microfluidic capture of circulating CD34<sup>+</sup> cells from unprocessed adult peripheral blood was compatible with the subsequent differentiation and culture of these cells into ECFCs with normal phenotypic identity and endothelial function. This validation was critical considering that other alternative (nonmicrofluidic) cytometric approaches have reportedly been found effective for the detection of ECFCs, but inadequate for the actual recovery of the cells.<sup>17</sup> Moreover, there exists the concern that flow cytometry may cause some degree of cell damage through acute hydrodynamic forces.<sup>18</sup> We also showed that, unlike with the standard methodology, separation of MNCs was not necessary for effective microfluidic capture and that the presence of erythrocytes did not interfere with the capturing process. Indeed, we were able to completely eliminate the need for density gradient centrifugation and erythrocyte lysis, both of which are laborious steps and are known to increase cell loss.

Our microfluidic approach was capable of providing enriched suspensions of CD34<sup>+</sup> cells in ~60 min from the time of blood withdraw, which is comparable to the processing time required in the standard method. However, unlike the standard method, the ability to run unprocessed blood through the microfluidic device enables the possibility of recirculating the CD34-depleted blood fraction back into the patient. In the clinics, this possibility would, in turn, facilitate processing a larger volume of blood without its complete withdrawal, which could be advantageous considering the low abundance of circulating ECFCs in adults.<sup>13</sup> Furthermore, our microfluidic technique is readily scalable; in the present study, each 6 mL of whole blood was directly flowed through 20 parallel microfluidic devices. However, there is no intrinsic limit to the number of devices that can be run in parallel to process larger volumes of peripheral blood. Collectively, we showed that the simplicity and versatility of microfluidic systems could be very instrumental in the isolation of ECFCs without compromising the biology and therapeutic potential of these cells.

The search for alternative methods to capture rare circulating cells with therapeutic potential remains an area of intense investigation in biomedical research.<sup>40,41</sup> In this field, fluorescence- and magnetic-activated cell sorting

(FACS and MACS, respectively) are still widely deemed as the gold standards.<sup>42</sup> Both FACS and MACS are well established and reliable and they usually provide purities >90%.<sup>43,44</sup> However, to date, no successful isolation of ECFCs has been reported using either FACS or MACS and thus the centrifugation method remains the standard. In addition, FACS still requires expensive instrumentation typically found only in core facilities. Also, both methods require labeling of cells with antibody tags, and in the case of FACS, centrifugation steps before cell separation, which notably increases the overall running time of the sorting process. Moreover, tagging cells with fluorescently labeled antibodies or magnetic particles remains a concern in certain applications. For example, it is unclear whether tagging circulating CD34<sup>+</sup> cells compromises subsequent differentiation of the capture cells into ECFCs.<sup>17</sup> Furthermore, magnetic labeling moieties have been shown to comprise viability and cellular function.<sup>45–47</sup> Fluorescent tags can pose similar concerns for cells that will ultimately be transplanted. By contrast, our microfluidic method did not require preprocessing labeling of the sample with fluorescent or magnetic tags or the associated incubation and centrifugation steps that may contribute to cell loss. Indeed, a key element in our devices was the use of an antibody-laden hydrogel coating that was originally designed to directly capture CD34<sup>+</sup> cells from undiluted whole blood,<sup>24</sup> and that we have now demonstrated can be effectively used to derive functional ECFCs from adults.

## Conclusion

In the present study, we demonstrated that microfluidic cell capture is an instrumental technology that can be effectively used for the isolation of rare circulating ECFCs from adult peripheral blood. We conducted preclinical experiments and unequivocally validated the phenotypic and functional properties of the captured human ECFCs, including the ability to form microvascular networks *in vivo*. We anticipate our results will facilitate additional development of clinically suitable microfluidic devices by the vascular therapeutic and diagnostic industry.

## Acknowledgments

This work was supported by the National Institutes of Health through grants R00EB009096 to J.M.-M. and R01EB009327 to S.K.M.

## Disclosure Statement

No competing financial interests exist.

## References

1. Melero-Martin, J., Khan, Z.A., Picard, A., *et al.* *In vivo* vasculogenic potential of human blood-derived endothelial progenitor cells. *Blood* **109**, 4761, 2007.
2. Kaushal, S., Amiel, G.E., Guleserian, K.J., *et al.* Functional small-diameter neovessels created using endothelial progenitor cells expanded *ex vivo*. *Nat Med* **7**, 1035, 2001.
3. Stroncek, J.D., Ren, L.C., Klitzman, B., and Reichert W.M. Patient-derived endothelial progenitor cells improve vascular graft patency in a rodent model. *Acta Biomater* **8**, 201, 2012.
4. Melero-Martin, J., De Obaldia, M.E., Kang, S.-Y., *et al.* Engineering robust and functional vascular networks

- in vivo* with human adult and cord blood-derived progenitor cells. *Circ Res* **103**, 194, 2008.
5. Traktuev, D.O., Prater, D.N., Merfeld-Clauss, S., *et al.* Robust functional vascular network formation *in vivo* by cooperation of adipose progenitor and endothelial cells. *Circ Res* **104**, 1410, 2009.
  6. Sipos, P.I., Bourque, S.L., Hubel, C.A., *et al.* Endothelial colony forming cells derived from pregnancies complicated by intrauterine growth restriction are fewer and have reduced vasculogenic capacity. *J Clin Endocrinol Metab* **98**, 4953, 2013.
  7. Baker, C.D., Black, C.P., Ryan, S.L., Balasubramaniam, V., and Abman, S.H. Cord blood endothelial colony-forming cells from newborns with congenital diaphragmatic hernia. *J Pediatr* **163**, 905, 2013.
  8. Ligi, I., Simoncini, S., Tellier, E., *et al.* A switch toward angiostatic gene expression impairs the angiogenic properties of endothelial progenitor cells in low birth weight preterm infants. *Blood* **118**, 1699, 2011.
  9. Borghesi, A., Massa, M., Campanelli, R., *et al.* Circulating endothelial progenitor cells in preterm infants with bronchopulmonary dysplasia. *Am J Respir Crit Care Med* **180**, 540, 2009.
  10. Ingram, D.A., Lien, I.Z., Mead, L.E., *et al.* *In vitro* hyperglycemia or a diabetic intrauterine environment reduces neonatal endothelial colony-forming cell numbers and function. *Diabetes* **57**, 724, 2008.
  11. Moreno-Luna, R., Muñoz-Hernandez, R., Lin, R.-Z., *et al.* Maternal body-mass index and cord blood circulating endothelial colony-forming cells. *J Pediatr* **164**, 566, 2014.
  12. Muñoz-Hernandez, R., Miranda, M.L., Stiefel, P., *et al.* Decreased level of cord blood circulating endothelial colony-forming cells in preeclampsia. *Hypertension* **64**, 165, 2014.
  13. Ingram, D.A., Mead, L.E., Tanaka, H., *et al.* Identification of a novel hierarchy of endothelial progenitor cells using human peripheral and umbilical cord blood. *Blood* **104**, 2752, 2004.
  14. Gulati, R., Jevremovic, D., Peterson, T.E., *et al.* Diverse origin and function of cells with endothelial phenotype obtained from adult human blood. *Circ Res* **93**, 1023, 2003.
  15. Yoder, M.C., Mead, L.E., Prater, D., *et al.* Redefining endothelial progenitor cells via clonal analysis and hematopoietic stem/progenitor cell principals. *Blood* **109**, 1801, 2007.
  16. Lin, Y., Weisdorf, D.J., Solovey, A., and Hebbel, R.P. Origins of circulating endothelial cells and endothelial outgrowth from blood. *J Clin Invest* **105**, 71, 2000.
  17. Mund, J.A., Estes, M.L., Yoder, M.C., Ingram, D.A., and Case, J. Flow cytometric identification and functional characterization of immature and mature circulating endothelial cells. *Arterioscler Thromb Vasc Biol* **32**, 1045, 2012.
  18. Mollet, M., Godoy-Silva, R., Berdugo, C., and Chalmers, J.J. Acute hydrodynamic forces and apoptosis: a complex question. *Biotechnol Bioeng* **98**, 772, 2007.
  19. Yoder, M.C. Is endothelium the origin of endothelial progenitor cells? *Arterioscler Thromb Vasc Biol* **30**, 1094, 2010.
  20. Van Beijnum, J.R., Rousch, M., Castermans, K., Der Linden Van, E., and Griffioen, A.W. Isolation of endothelial cells from fresh tissues. *Nat Protoc* **3**, 1085, 2008.
  21. El-Ali, J., Sorger, P.K., and Jensen, K.F. Cells on chips. *Nature* **442**, 403, 2006.
  22. Plouffe, B.D., Njoka, D.N., Harris, J., *et al.* Peptide-mediated selective adhesion of smooth muscle and endothelial cells in microfluidic shear flow. *Langmuir* **23**, 5050, 2007.
  23. Plouffe, B.D., Kniazeva, T., Mayer, J.E., Murthy, S.K., and Sales, V.L. Development of microfluidics as endothelial progenitor cell capture technology for cardiovascular tissue engineering and diagnostic medicine. *FASEB J* **23**, 3309, 2009.
  24. Hatch, A., Hansmann, G., and Murthy, S.K. Engineered alginate hydrogels for effective microfluidic capture and release of endothelial progenitor cells from whole blood. *Langmuir* **27**, 4257, 2011.
  25. Zhu, B., Smith, J., Yarmush, M.L., *et al.* Microfluidic enrichment of mouse epidermal stem cells and validation of stem cell proliferation *in vitro*. *Tissue Eng Part C Methods* **19**, 765, 2013.
  26. Hatch, A., Pesko, D.M., and Murthy, S.K. Tag-free microfluidic separation of cells against multiple markers. *Anal Chem* **15**, 4618, 2012.
  27. Hansmann, G., Plouffe, B.D., Hatch, A., *et al.* Design and validation of an endothelial progenitor cell capture chip and its application in patients with pulmonary arterial hypertension. *J Mol Med* **89**, 971, 2011.
  28. Lin, R.-Z., Dreyzin, A., Aamodt, K., *et al.* Induction of erythropoiesis using human vascular networks genetically engineered for controlled erythropoietin release. *Blood* **118**, 5420, 2011.
  29. Lin, R.-Z., and Melero-Martin, J. Bioengineering human microvascular networks in immunodeficient mice. *J Vis Exp* **11**, e3065, 2011.
  30. Yoder, M.C. Human endothelial progenitor cells. *Cold Spring Harb Perspect Med* **2**, a006692, 2012.
  31. Yoder, M.C. Endothelial progenitor cell: a blood cell by many other names may serve similar functions. *J Mol Med* **91**, 285, 2013.
  32. Asahara, T., Murohara, T., Sullivan, A., *et al.* Isolation of putative progenitor endothelial cells for angiogenesis. *Science* **275**, 964, 1997.
  33. Shi, Q., Rafii, S., Wu, M.H., *et al.* Evidence for circulating bone marrow-derived endothelial cells. *Blood* **92**, 362, 1998.
  34. Fadini, G.P., Losordo, D., and Dimmeler, S. Critical re-evaluation of endothelial progenitor cell phenotypes for therapeutic and diagnostic use. *Circ Res* **110**, 624, 2012.
  35. Hur, J., Yoon, C.-H., Kim, H.-S., *et al.* Characterization of two types of endothelial progenitor cells and their different contributions to neovasculogenesis. *Arterioscler Thromb Vasc Biol* **24**, 288, 2004.
  36. Au, P., Daheron, L.M., Duda, D.G., *et al.* Differential *in vivo* potential of endothelial progenitor cells from human umbilical cord blood and adult peripheral blood to form functional long-lasting vessels. *Blood* **111**, 1302, 2008.
  37. Reinisch, A., Hofmann, N., Obenauf, A., *et al.* Humanized large-scale expanded endothelial colony-forming cells function *in vitro* and *in vivo*. *Blood* **113**, 6716, 2009.
  38. Lin, R.-Z., Chen, Y.-C., Moreno-Luna, R., Khademhosseini, A., and Melero-Martin, J. Transdermal regulation of vascular network bioengineering using a photopolymerizable methacrylated gelatin hydrogel. *Biomaterials* **34**, 6785, 2013.
  39. Asahara, T., Kawamoto, A., and Masuda, H. Concise review: circulating endothelial progenitor cells for vascular medicine. *Stem Cells* **29**, 1650, 2011.
  40. Mattanovich, D., and Borth, N. Applications of cell sorting in biotechnology. *Microb Cell Fact* **21**, 12, 2006.
  41. Autebert, J., Coudert, B., Bidard, F.-C., *et al.* Microfluidic: an innovative tool for efficient cell sorting. *Methods* **57**, 297, 2012.

42. Ibrahim, S.F., and van den Engh, G. High-speed cell sorting: fundamentals and recent advances. *Curr Opin Biotechnol* **14**, 5, 2003.
43. Pappas, D., and Wang, K. Cellular separations: a review of new challenges in analytical chemistry. *Anal Chim Acta* **601**, 26, 2007.
44. Zborowski, M., and Chalmers, J.J. Rare cell separation and analysis by magnetic sorting. *Anal Chem* **83**, 8050, 2011.
45. Liu, G., Gao, J., Ai, H., and Chen, X. Applications and potential toxicity of magnetic iron oxide nanoparticles. *Small* **9**, 1533, 2013.
46. Sharifi, S., Behzadi, S., Laurent, S., *et al.* Toxicity of nanomaterials. *Chem Soc Rev* **41**, 2323, 2012.
47. Soenen, S.J., Rivera-Gil, P., Montenegro, J.M., *et al.* Cellular toxicity of inorganic nanoparticles: common aspects and guidelines for improved nanotoxicity evaluation. *Nano Today* **6**, 446, 2011.

Address correspondence to:  
*Juan M. Melero-Martin, PhD*  
*Department of Cardiac Surgery*  
*Boston Children's Hospital*  
*300 Longwood Ave., Enders 349*  
*Boston, MA 02115*

*E-mail:* [juan.meleromartin@childrens.harvard.edu](mailto:juan.meleromartin@childrens.harvard.edu)

*Received:* June 23, 2014

*Accepted:* July 30, 2014

*Online Publication Date:* September 16, 2014

**This article has been cited by:**

1. Janay Elise Kong, Soroush Kahkeshani, Ivan Pushkarsky, Dino Di Carlo. 2014. Research highlights: micro-engineered therapies. *Lab Chip* 14, 4585-4589. [[CrossRef](#)]